#### **Research Article**

Natesan Karthikeyan, Jesuarockiam Naveen\*, Murugan Rajesh, Degalhal Mallikarjuna Reddy, P. Edwin Sudhagar, Mohd Nor Faiz Norrrahim\*, and Victor Feizal Knight

# Flexural and vibration behaviours of novel covered CFRP composite joints with an MWCNT-modified adhesive

https://doi.org/10.1515/ntrev-2024-0076 received May 14, 2024; accepted July 14, 2024

Abstract: Co-curing bonding is more efficient than cobonding and secondary bonding for structural component assembly. This work used novel covered laminas with cocured joining techniques (CL-CCT) to create carbon fibre-reinforced polymer (CFRP) composite adhesive-bonded joints. Additionally, the researchers evaluated how multi-walled carbon nanotubes (MWCNTs) affect the bending and dynamic properties of CFRP composite joints. The researchers added various weights of MWCNTs to the covered laminas along with co-cured CFRP adhesive-bonded joints. The study revealed that epoxy and 0.25 wt% MWCNT adhesive produced the strongest and most flexible joints. These joints were 118 and 15% stronger than joints made from pure epoxy CL-CC CFRP, respectively. Compared to pure epoxy CC-CFRP composite joints, the strength of CL-CC CFRP composite joints with 0.25 wt% MWCNTs increased by 374 and 109%, respectively. Interestingly, MWCNTs with a wt% of 1.25 had the greatest natural frequency in all three vibration modes, which are 19, 19, and 13% higher than that of the pure epoxy CL-CC CFRP composite joint. There are 28, 30, and 24% more natural frequencies in 1.25 wt% MWCNT-based CL-CC CFRP composite joints than those in pure epoxy-based joints in all three modes. Analysis of variance was employed for

statistical investigation. Optimization and prediction were done using an artificial neural network and the Levenberg–Marquardt technique.

**Keywords:** CFRP composite joints, covered laminas, MWCNTs, ANOVA, and ANN

artificial neural network

# **Acronyms**

ANN

ANOVA	analysis of variance
CC-CFRP	co-cured carbon fibre-reinforced polymer
CFRP	carbon fibre-reinforced polymer
CL-CC-CFRP	covered lamina with co-cured carbon fibre-
	reinforced polymer
CL-CCT	covered lamina with co-cured joining
	techniques
FESEM	field emission scanning electron microscopy
FRP	fibre-reinforced polymer
GFRP	glass fibre-reinforced polymer
GNPs	graphene nanoplatelets
MWCNTs	multiwalled carbon nanotubes
SLJ	single lap joint

Natesan Karthikeyan, Murugan Rajesh, Degalhal Mallikarjuna Reddy, P. Edwin Sudhagar: School of Mechanical Engineering, Vellore Institute of Technology, Vellore, 632014, Tamil Nadu, India

**Victor Feizal Knight:** Research Center for Chemical Defence, Defence Research Institute (DRI), Universiti Pertahanan Nasional Malaysia, Kem Sungai Besi, 57000, Kuala Lumpur, Malaysia

# 1 Introduction

Lightweight applications like aerospace, marine, and automobiles have greatly benefited from fibre-reinforced polymer (FRP) composite structures [1–4]. For large-scale manufacturing, joining techniques are unavoidable. Various traditional joining techniques such as bolted, riveted, and welded joints have more drawbacks such as localized stress, higher fatigue life, weight addition, and delamination while using mechanical fasteners. The adhesive-bonded joints have overcome the problems of traditional bonding techniques [5–8]. In aerospace applications, this bonding method is used in

<sup>\*</sup> Corresponding author: Jesuarockiam Naveen, School of Mechanical Engineering, Vellore Institute of Technology, Vellore, 632014, Tamil Nadu, India, e-mail: naveen.j@vit.ac.in

<sup>\*</sup> Corresponding author: Mohd Nor Faiz Norrrahim, Research Center for Chemical Defence, Defence Research Institute (DRI), Universiti Pertahanan Nasional Malaysia, Kem Sungai Besi, 57000, Kuala Lumpur, Malaysia, e-mail: faiz@upnm.edu.my

2 — Natesan Karthikeyan *et al.* DE GRUYTER

various composite parts in wings, fuselages, and frames [9]. The mechanical performance of the adhesive-bonded joints considered the following factors such as the joining method [2,3,10–13], surface treatment [14–23], type of the matrix used [9,21,24], matrix modification by nanofillers [3,10,12,23–30], and additional reinforcement with adhesives [1,2,10,12,13,31–33]. The development of adhesive-bonded techniques and adhesions was driven by the need to manufacture components on a large scale.

There are various types of adhesive-bonded joining methods such as secondary bonding, co-bonding, co-curing, and multi-material bonding [2–4.11.12]. Secondary bonding techniques joined two cured laminates. The co-bonding technique joined one cured laminate to another uncured laminate. Co-cured composite joints were one of the joining methods for FRP adhesively bonded joints, which involved joining both uncured laminates. Co-cured composite joints have higher strength and durability than secondary bonding methods. This method enables seamless integration of the two laminates, resulting in a stronger overall bond. In addition, co-cured composite joints are a more efficient and costeffective way to join laminates than secondary bonding methods. Furthermore, this technique reduces the likelihood of delamination or separation of the two materials over time. Furthermore, in co-curing joining methods, there is no need for additional surface treatment methods. The multi-material bonding process is used to join cured dissimilar composites and metals.

The composite material consists of a combination of the glass fibre-reinforced polymer (GFRP) and carbon nanotubes (CNTs), which together make up approximately 0.25% of the material's weight. The composite joint exhibits a resonance frequency of 53.1 Hz and a shear strength of 16.73 MPa in Mode 1 [11,12]. Similarly, 0.75 wt% of GNP and 2.5 vol% of 90°/Z-pins + 0.75 wt% GNP-based adhesives in GFRP composite joints have attained the shear strength of 13.10 and 17.83 MPa, respectively [34]. Research has shown that incorporating steel Z-pins into the matrix significantly enhances the fracture resistance of co-cured carbon fibre-reinforced polymer (CFRP) composite joints [31]. Quan et al. used surface-treated CF/PEEK tape-based adhesive to create the cocured CFRP composite joints, which had shear strengths of 27 and 25 MPa at 22 and 130°C, respectively [35]. The effects of adherends modified on the surface and adhesives modified with a nanofiller on the shear behaviour of secondarybonded and co-bonded single-lap joints were reviewed by Karthikevan and Naveen [4]. Additionally, they talked about how different nanofiller adhesives in the FRP composite and dissimilar composite single-lap joints are affected by different mechanical properties [1]. Incorporating multi-walled carbon nanotubes (MWCNTs) can enhance various properties,

including tensile modulus, tensile strength, flexural strength, interlaminar shear strength (ILSS), toughness, damping behaviour, and glass transition temperature. At specified stirring times, the flexural strength of the treated MWCNTs-CFRP laminates is 948 MPa, while the ILSS is 66.7 MPa [36]. The incorporation of glass powder into a co-cured glass fibre-reinforced polymer composite resulted in a substantial improvement in its mechanical properties. Specifically, there was a substantial rise in both the flexural and shear strengths, increasing from 19.31 to 208.92 MPa. In addition, the natural frequency of the composite in Mode-3 increased to 881.3 Hz [37]. The statistical analysis utilized the one-way analysis of variance (ANOVA) method to evaluate the error rate and the impact of different inputs on the output parameters of the composites [22,38,39]. The genetic algorithm, artificial neural network (ANN), and Levenberg-Marquardt algorithm were collectively employed to optimize and forecast the outcomes of the joints and composites [22,33,38-41]. A thorough examination of the composite materials was conducted using advanced optimization techniques, resulting in substantial enhancements to their mechanical properties.

After carefully examining the literature, several significant findings were uncovered. Numerous studies have been conducted to analyse the shear, flexural, and vibrational properties of co-cured GFRP composite joints that incorporate an adhesive enhanced with MWCNTs. There is currently a limited amount of research available on the flexural and vibration properties of co-cured CFRP composite joints that use adhesives enhanced with MWCNTs. This study examined the impact of MWCNTs on the dynamic and flexural characteristics of novel covered laminas with cocured carbon fibre-reinforced polymer (CL-CC CFRP) composite joints. In addition, the JMP Pro 17 software will be used to perform a one-way ANOVA to investigate any significant differences in the results. Utilizing an ANN and MATLAB software, the performance and prediction model for forecasting future outcomes is finely tuned.

# 2 Materials and methods

#### 2.1 Materials

SM Composites in Chennai, India, provided the bi-directional woven carbon fabric with an area weight and thickness of 220 g/m<sup>2</sup> and 0.40 mm, respectively. MWCNTs were acquired from BTCORP Generique Nano Pvt Ltd in Bangalore. The properties of MWCNTs are 20 nm in diameter, 20 µm in length, >99% purity, 220 m<sup>2</sup>/g specific surface area, and 0.16 g/cm<sup>3</sup>

bulk density. SM Composites in Chennai, India, supplied the epoxy resin [LY556] and the triethylenetetramine araldite epoxy hardener [HY951].

# 2.2 MWCNT dispersion method

The process of spreading MWCNTs in epoxy is shown in Figure 1, which describes the technique. In the beginning, a precise weighing device was used to ascertain the various weight proportions of MWCNT particles. The weight percentages of 0.25, 0.5, 0.25, 0.75, 1.0, 1.25, and 1.5 were given attention, and observations were made about them. After that, the MWCNTs were combined in a beaker that previously had 100 g of acetone that was in its purest form. The beaker was subjected to ultrasonication for 1h in an ultrasonicator, with the frequency ranging from 30 to 40 kHz. A mixture that contained approximately 50% acetone was obtained as a consequence of the sonication process, which resulted in the vaporization of approximately 50% of the acetone. The mixture was then subjected to an extra round of sonication after a required quantity of epoxy was added to the MWCNT/acetone mixture and mixed well. After that, acetone is present in the epoxy/MWCNT composite mixture in proportions that have been accurately calculated. During the process of extracting the acetone from the liquid, a magnetic stirrer was used to swirl the liquid at a speed of 900 revolutions per minute, while the temperature was maintained at 60°C. In the end, the adhesive formed a uniform combination of MWCNTs and epoxy, resulting in improved bonding of single-lap joints [1–4,12,13,26,27,42].

# 2.3 Uncured laminate preparation

An uncured CFRP composite was fabricated by combining the epoxy resin and hardener in a weight ratio of 10:1. First, manufacturing of the four-ply CFRP laminates was carried out using the manual process of hand layup, which is the recommended method. The CFRP laminates have a matrix and fibre weight ratio of 50/50. To remove any excess resin, the laminates that had not yet solidified were subjected to vacuum sealing and crushed at a pressure of 1 bar for 30 min [2,3,11–13,27]. Figure 2 depicts a diagrammatic representation of the vacuum bag moulding process.

# 2.4 CL-CC-CFRP composite joint preparation

The study involved fabricating adhesive-bonded CFRP singlelap joint samples using co-curing adhesive-bonding methods.

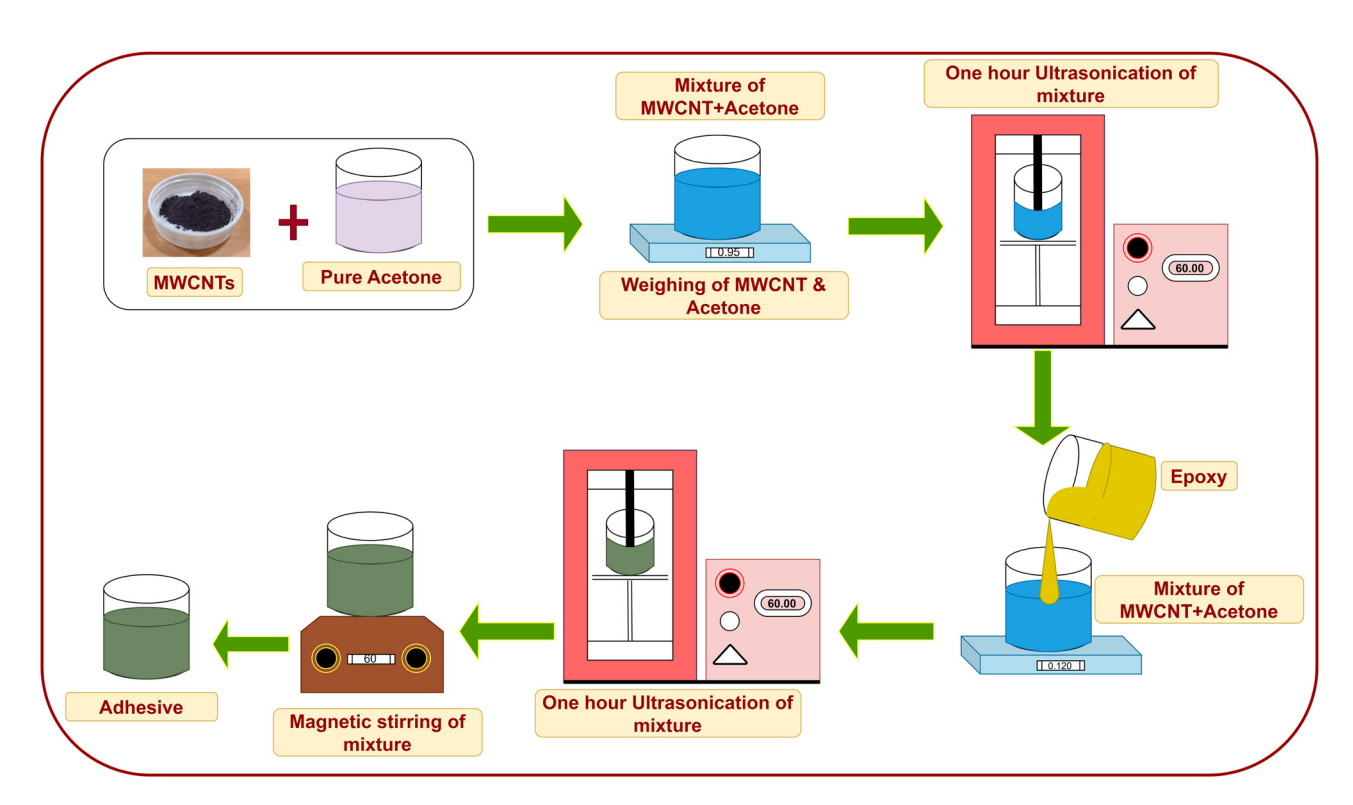


Figure 1: MWCNT/epoxy adhesive preparation using the MWCNT dispersion process.

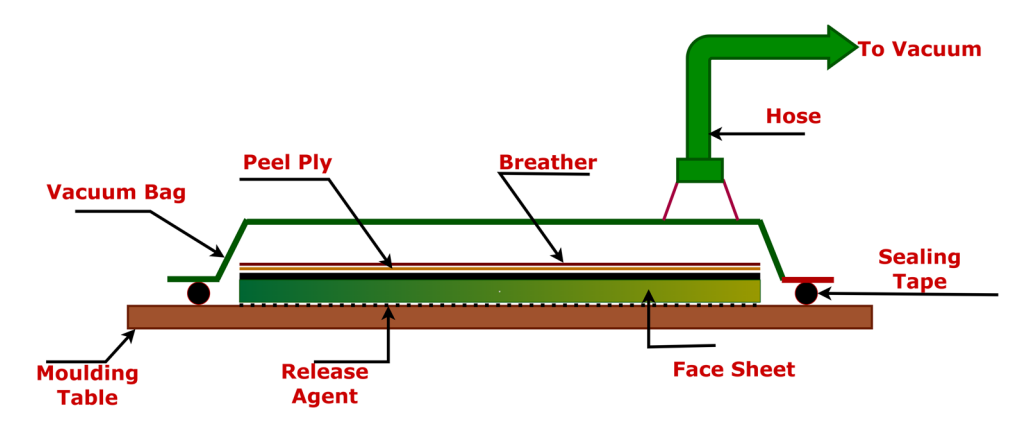


Figure 2: Schematic diagram of the vacuum bag moulding process.

Figure 3 displays an accomplished single-lap connection made with CFRP composites using the co-curing bonding technique. A specially designed mould maintained the adhesive thickness in the CFRP single-lap joint at 0.5 mm. The top and bottom wood control plates and support plates, each measuring 3 mm in thickness, comprised the custom mould. The four-layer uncured CFRP composite specimens were arranged with overlapping gaps of 25.4 mm. There is a fifth and sixth lamina covered on both sides of the single lap joints. Figure 4(a)–(c) presents a

custom-made mould, highlighting the covered lamina with CFRP single lap joint configuration. The adhesive, made up of MWCNTs and pure epoxy, was combined with a hardener using a weight ratio of 10:1. The adhesive was applied to both the regions of overlap and the covered lamina of the joints. With precision, the thickness control plate measures the adhesive thickness in the overlap zone at a precise value of 0.5 mm. Following their preparation, the composite joints underwent a two-step curing process. Initially, they were

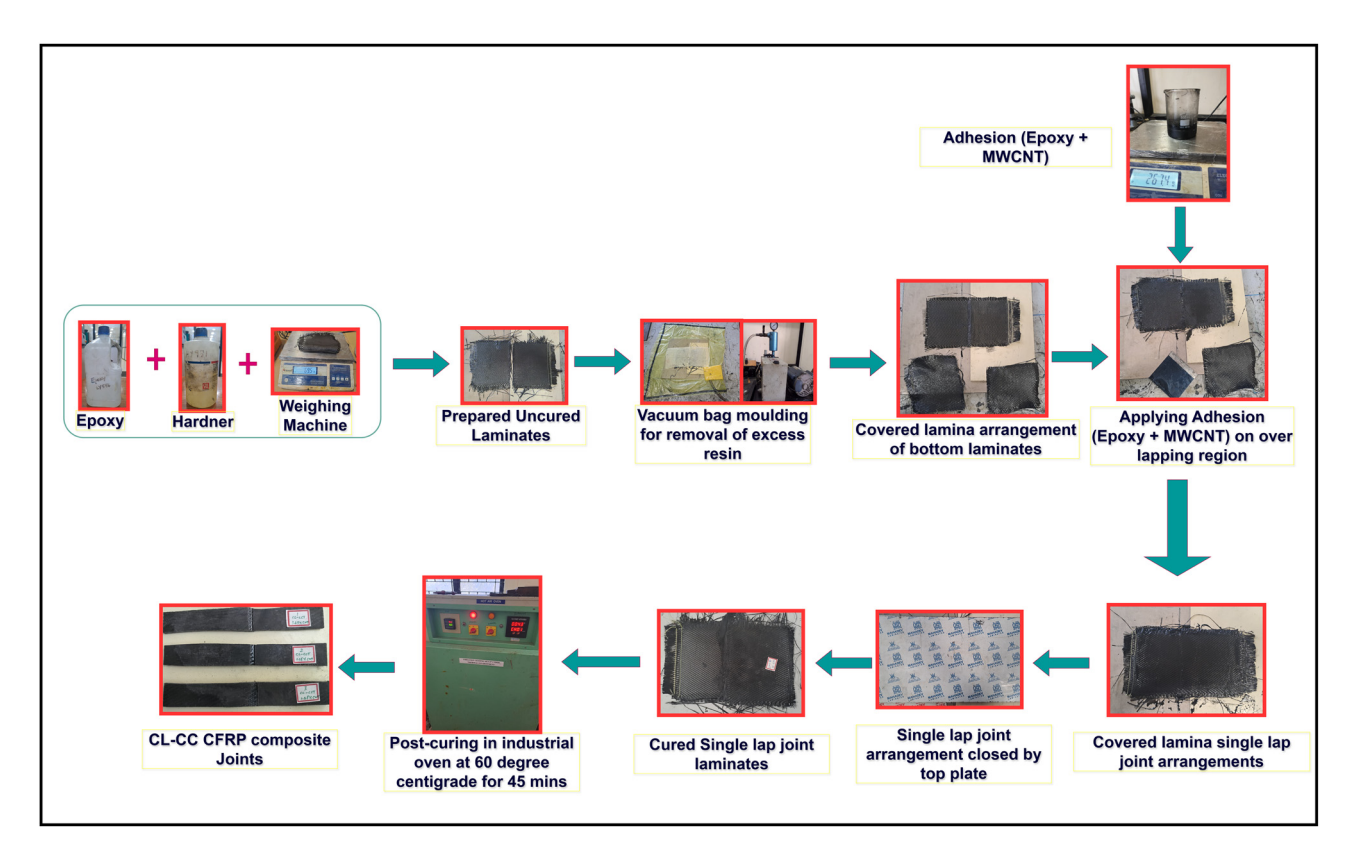


Figure 3: CFRP single lap joint fabrication process.

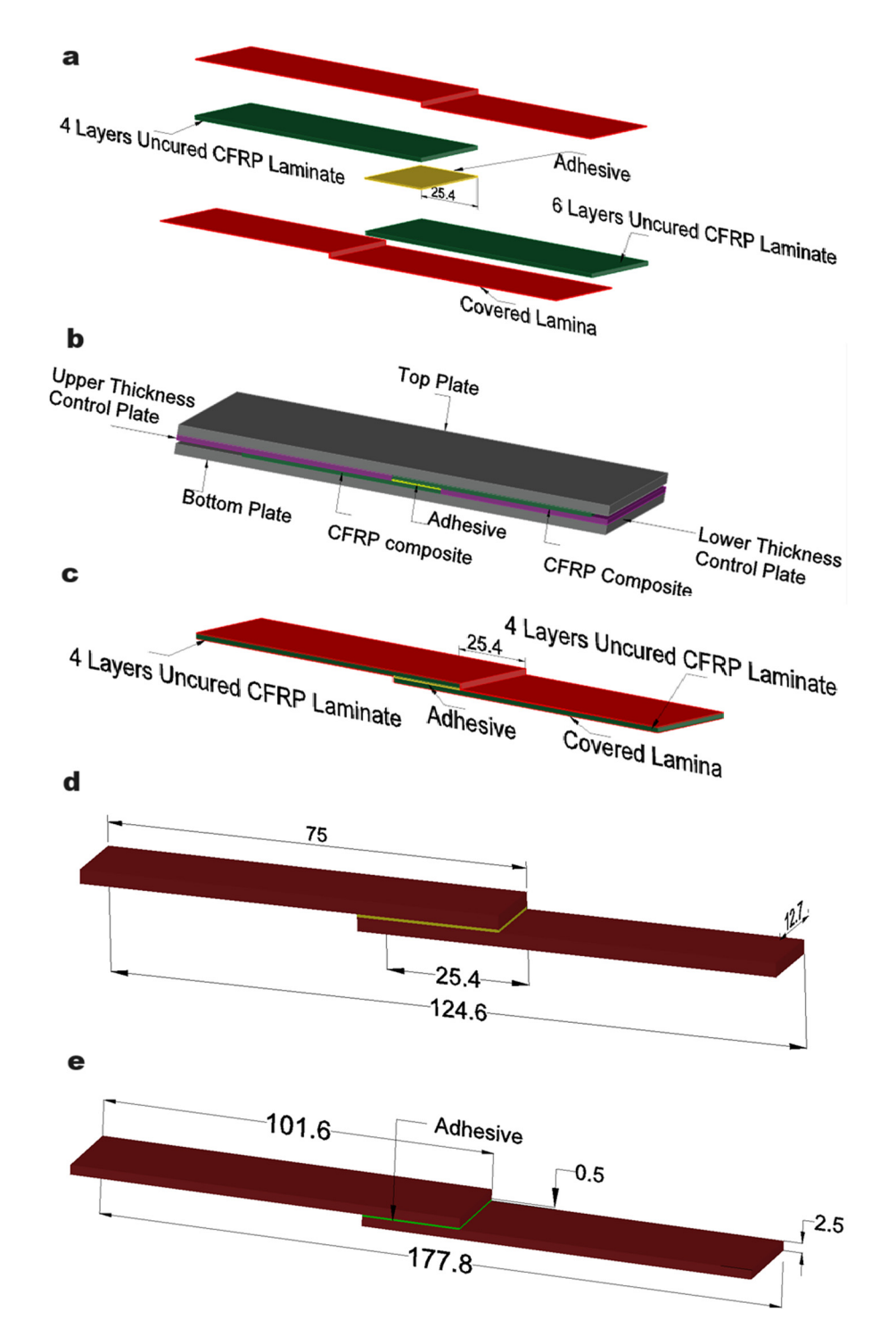


Figure 4: Fabrication technique: (a) arrangement of adherends, (b) a specially designed mould, (c) single lap joint, (d) flexural test sample dimensions, and (e) vibration test sample dimensions.

placed in a controlled environment for an entire day. Following that, they were transferred to an industrial oven set at a temperature of 60°C and left for 45 min. The flexural and vibration test sample dimensions were set following the specifications provided by ASTM D 790 and ASTM D 5868, respectively, which are illustrated in Figure 4(d) and (e).

# 2.5 Testing procedures

#### 2.5.1 Flexural testing

The H10KL universal testing equipment, manufactured by Tinius Olsen, was employed to perform a flexural test under normal room temperature conditions. Figure 5(a) illustrates a schematic representation of a flexural test specimen for covered laminas with co-cured joining techniques (CL-CCT) CFRP composite single lap joints that is attached to the UTM machine fixture. This joint was produced in compliance with the specifications established by ASTM D 790. Three specimens were used for the flexural test, with each specimen representing a different weight percentage. The loading rate in this experiment was consistently maintained at 2 mm/min. In Figure 5(b), a specimen is loaded and then subjected to a flexural test.

To examine the values of flexural stress and flexural strain on the adhesive joints, equations (1) and (2) were used.

$$\sigma_{\rm f} = \frac{3WL}{2bd^2},\tag{1}$$

where  $\sigma_f$  is the flexural stress at the midpoint in MPa, W is the load at the midpoint, L is the span of support in mm, b is the joint's width (mm), and d is the joint's depth in mm.

$$\varepsilon_{\rm f} = \frac{6Dd}{L^2},\tag{2}$$

where  $\varepsilon_{\rm f}$  represents the midpoint flexural strain in mm/mm and D is the displacement measured in mm at the joint's centre.

#### 2.5.2 Free vibration testing

This study investigates the impact of varying weight percentages of MWCNTs on the inherent vibration characteristics of CL-CCT CFRP composite single-lap joints. The joints were created using a co-curing bonding process. A study was conducted to investigate the occurrence of free vibrations with fixed-free boundary conditions, utilizing three replicates of samples. An analysis was performed on the first three mode shapes to calculate the natural frequency of the CL-CCT CFRP single-lap joint samples. The CFRP

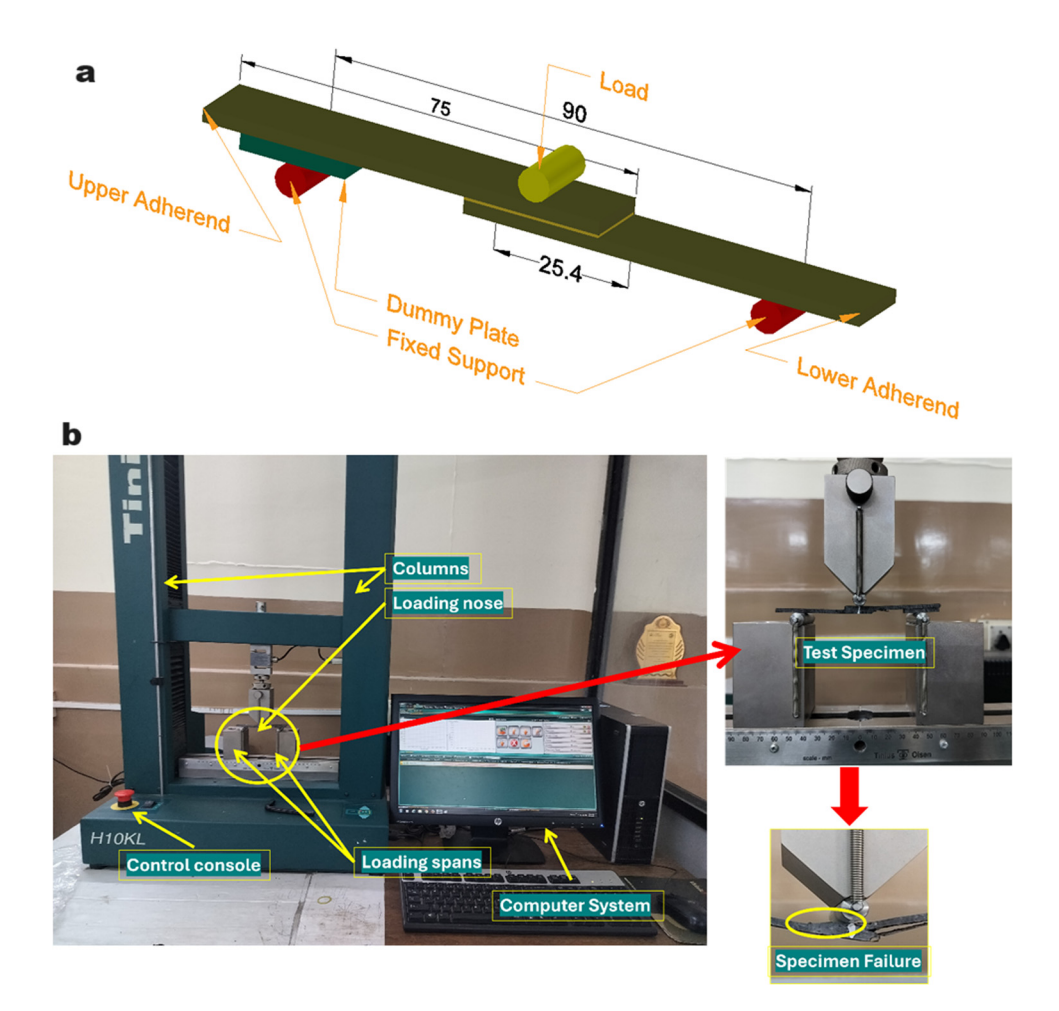


Figure 5: (a) Flexural test specimen and (b) flexural test setup under loading conditions.

composite junction was firmly attached to a stationary support at one end. Figure 6(a and b) illustrates the procedure of applying excitations using a Dytran (5800SL) impulse hammer, which has a sensitivity of 23.493 mV/N. Having been attached to the composite joint, a highly sensitive accelerometer (352C22/NC) with a sensitivity of 10.54 mV per g was utilized to gather the impact signal. The time–domain data were analysed using a fast Fourier transform with a data-collecting device that has four channels and a sampling rate of 52.13 kg samples per second. It accurately determined the natural frequency of composite joints using the DEWE software.

A Nyquist plot was generated using the circle fit technique to determine the damping ratio of the mode. The primary benefit of this method was a diminished impact on the ultimate result, achieved by decreasing the number of locations around the primary point of response and its intensity. A benefit of the half-power band approach is its ability to precisely compute the damping ratio, regardless

of the proximity of the mode frequencies. Upon using the circle fit technique on the resonance peak data, it became evident that the data points were arranged circularly [43]. The damping value can be determined by using the circle fit method and applying the following formula:

$$\zeta = \frac{\omega_2^2 - \omega_1^2}{2\omega_0 \left[\omega_2 \tan \frac{\alpha_2}{2} + \omega_1 \tan \frac{\alpha_1}{2}\right]},$$
 (3)

where  $\omega_0$  implies the angular frequency at resonance,  $\alpha_1$  and  $\alpha_2$  denote the angle between angular frequencies, respectively, and  $\omega_1$  and  $\omega_2$  denote the angular frequencies, respectively [44].

#### 2.5.3 Morphology testing

An FEI Quanta 250 FEG, a Thermo Fisher field emission scanning electron microscopy (FE-SEM) apparatus, was

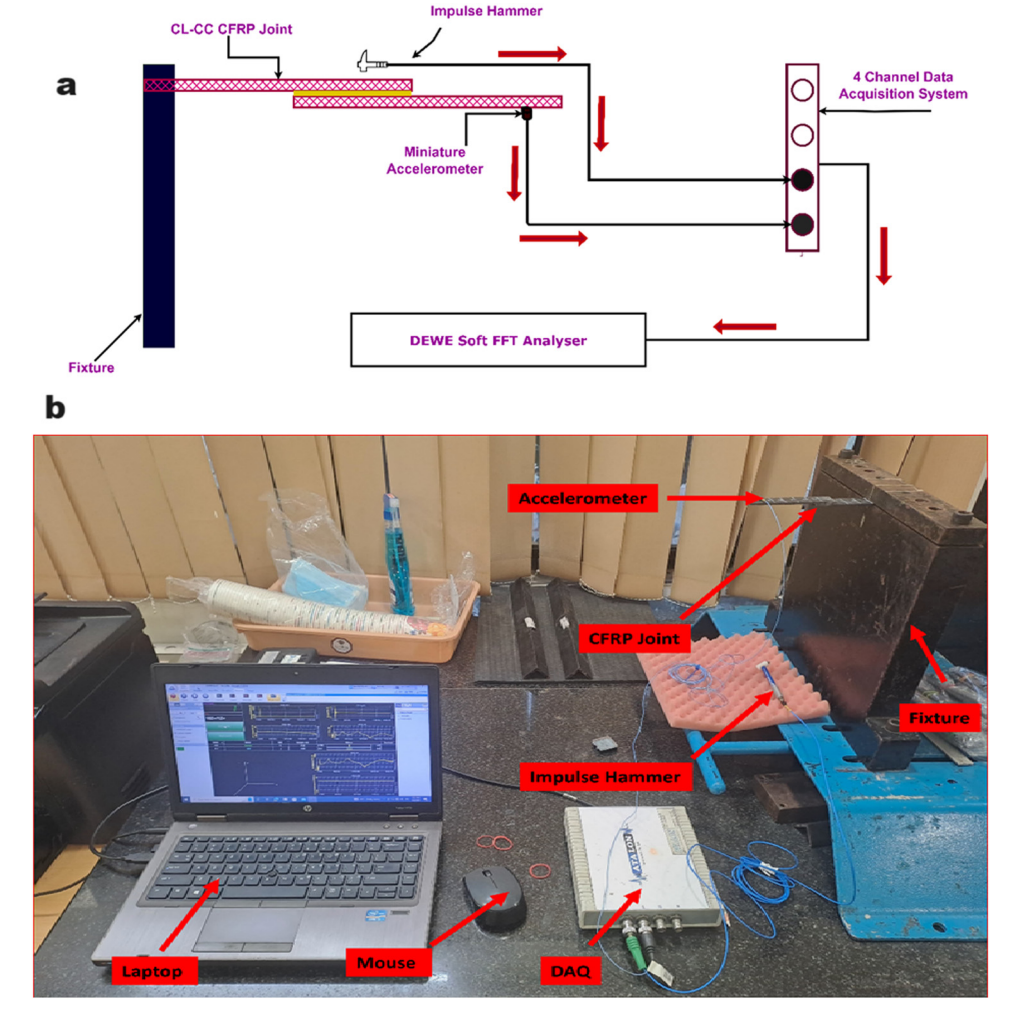


Figure 6: (a) Schematic diagram of the vibration test and (b) experimental vibration test setup with the CFRP joint specimen.

8 — Natesan Karthikeyan *et al.* DE GRUYTER

employed to examine the morphological characteristics of the fractured surface of single lap joints. The device obtains its principal electron supply from a Schottky field emission electron cannon. The features of this instrument are truly unique and unparalleled. The device operates within a voltage range of 5-30 kV and attains a magnification of 100,000× when employed in a high vacuum environment at 30 kV. Following the failure of flexural surface samples, the fractography of those samples was performed using a field emission scanning electron microscope. The primary aim was to ascertain the exact mechanism by which the fracture occurred. Prior to analysis, the specimens underwent resizing using a specialized cutting instrument to achieve dimensions of 10 mm × 10 mm × 2.5 mm. In order to enhance the electrical conductivity of the surfaces. a preparatory layer of gold was folio-coated.

# 3 Results and discussion

# 3.1 Flexural analysis

The flexural performance of adhesive-bonded joints in CL-CC CFRP composites has been improved by adding different weight percentages (0.25, 0.5, 0.75, 1.0, 1.25, and 1.5) of MWCNTs. The experimental data demonstrate the impact of MWCNTs on stress-strain, as shown in Figure 7(a). The addition of MWCNTs to the epoxy adhesive significantly enhances the energy-absorbing capabilities of composite joints, as shown in Figure 7(b). The outcome is a catastrophic collapse of a CL-CC CFRP junction with only epoxy as a bond, experimentation of which is proven to be true. MWCNTs have been included in epoxy adhesives to enhance their linear elasticity. The material's capacity is enhanced to inhibit the initiation and propagation of matrix fractures. The addition of MWCNTs to the adhesive helps reduce the formation of concentrated stress when subjected to bending loads. It is well recognized that tension in fibres is less prone to debonding or failure when it is uniformly distributed. The research demonstrated that the adhesive containing MWCNTs exhibited significantly enhanced adhesion compared to the pure adhesive. The flexural strength of a composite joint made only of adhesive-based CL-CC CFRP is 231 MPa. The pure epoxy adhesive was modified with different concentrations of MWCNTs, namely, 0.25, 0.5, 0.75, 1.00, 1.25, and 1.5%. The flexural strength values for each concentration were found under the flexural loading. The findings indicated that the inclusion of 0.25% by weight of MWCNT resulted in a substantial

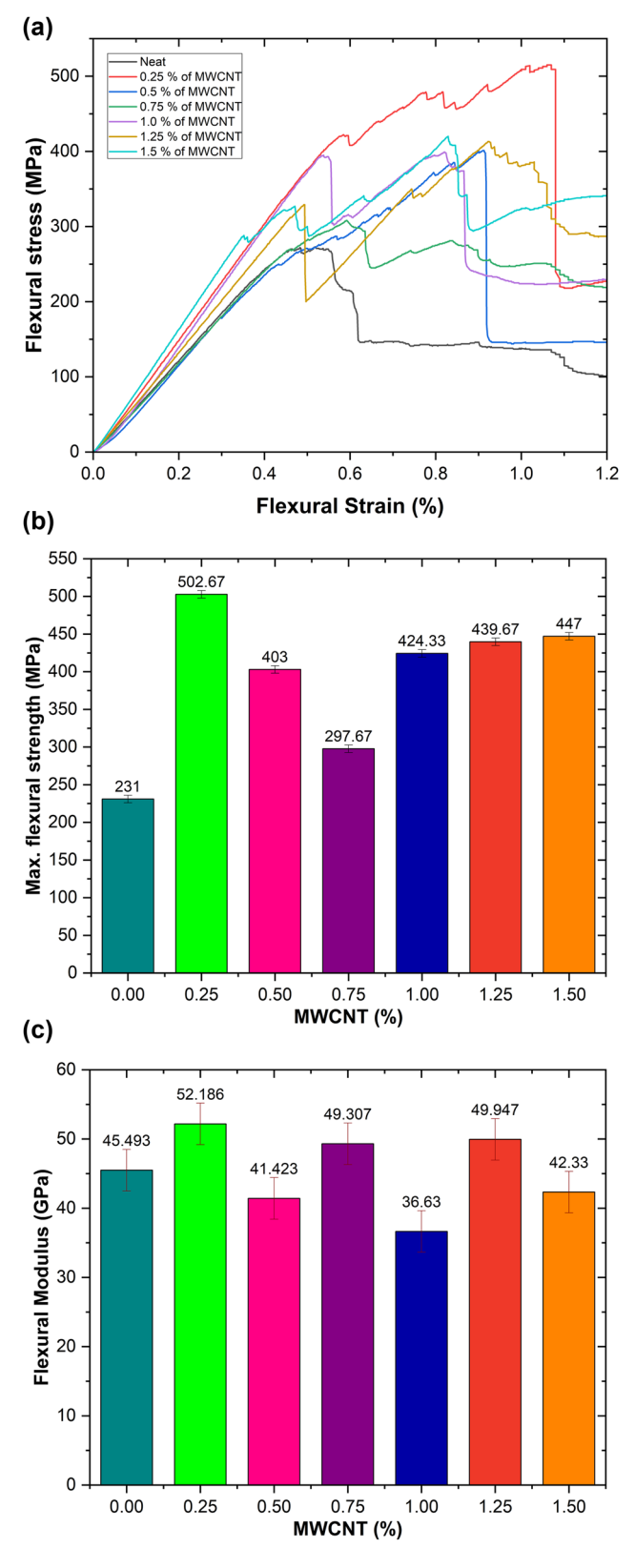


**Figure 7:** (a) Flexural stress *versus* flexural strain, (b) flexural strength *versus* wt% of MWCNT content, and (c) flexural modulus *versus* wt% of MWCNT content.

enhancement in the flexural strength of the epoxy. The greatest value achieved was 502 MPa, representing a 118% increase compared to the pure epoxy adhesive.

Composite joints' flexural modulus is substantially enhanced when MWCNTs are added to epoxy adhesive, as shown in Figure 7(c). The research showed that adding 0.25% MWCNTs by weight significantly increased the epoxy's flexural modulus, reaching a maximum of 52.19 GPa. On the other hand, the strength of this material is 15% more than that of pure epoxy. The adhesive's spreading and adhesion capabilities are diminished, and its viscosity increases with larger nanoparticle concentrations, both of which degrade the adherence. Additionally, due to their enormous surface area, nanoparticles have a tendency to aggregate, which causes tension to accumulate at the aggregated particles and a subsequent weakening of the material. A coarse surface developed on the adhesive layer, which increased its strength. Because of this layer, the glue was able to cling to the substrate much better. As a result, the usual joint's resistance to bending stress was much improved [27]. Compared with the previous research work by the same author, the flexural strength and modulus of pure epoxy-based CL-CC CFRP composite joints exhibit a significant increase compared to those of pure epoxy CC-CFRP composite joints which is 118 and 91%, respectively. In comparison, the CL-CC CFRP composite joints with 0.25 wt% of MWCNTs show a significant increase of 374 and 109% compared to the pure epoxy CC-CFRP composite joints. Based on these findings, it has been observed that the covered lamina effectively functions as a load-bearing reinforcement when subjected to flexural load in the CFRP composite joints.

The load-displacement curves depict the bending load that leads to the failure of these joints made of CFRP composites, which is illustrated in Figure 8. When a flexural load is applied to the CL-CC CFRP composite joints, both the covered lamina and adhesive initially resist the load. Subsequent loading results in the initial failure occurring on both sides of the covered lamina in the overlapped region. At that moment, the load abruptly dropped without any deformation. Furthermore, the adhesive has the ability to endure further stress until it eventually breaks. The hand layup technique is used to construct joints to accommodate changing flexural stress and modulus, leading to varying composite thickness. Excessive quantities of adhesive containing MWCNTs lead to specimen slippage during testing, which in turn affects the point where the load is applied. To reduce the occurrence of specimen slips, it is advised to exercise meticulous control over the quantity of MWCNT-based glue used during the manufacturing process. In addition, maintaining a constant load application point throughout testing will aid in correctly evaluating the performance of the joints at varying levels of bending stress and modulus.

# 3.2 Vibrational behaviour analysis

Figure 9(a)–(c) displays the experimental examination of the natural frequencies of Mode-1, Mode-2, and Mode-3 in MWCNTs reinforced with adhesive-based CFRP composite joints, conducted by a free vibration test. The damping factor of the tested samples in three modes is shown in

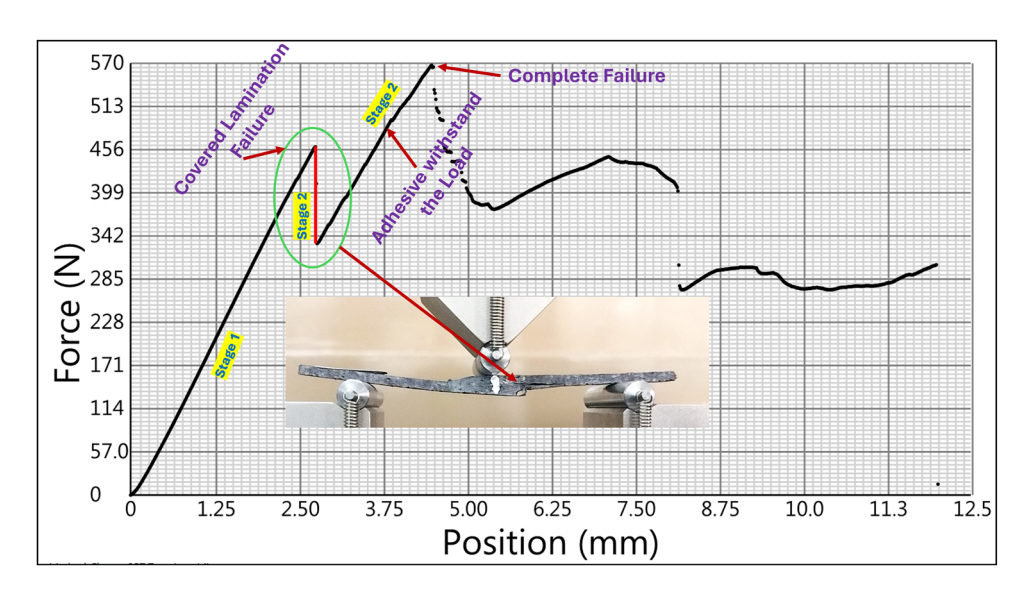
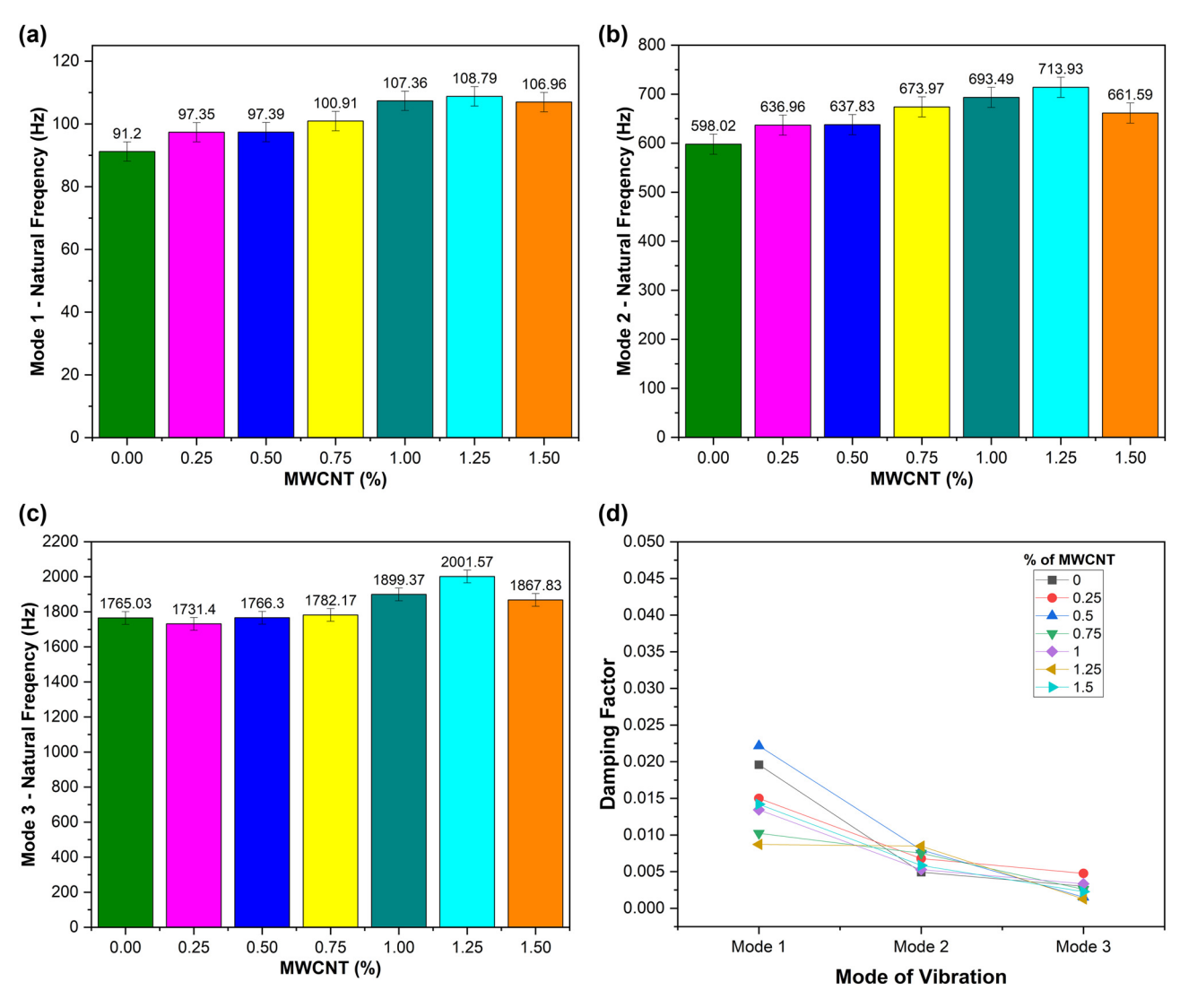


Figure 8: Failure mode of the CL-CC CFRP composite joint under flexural loading.

Figure 9(d). The CFRP composite joint specimen, bonded with pure epoxy adhesive, demonstrates natural frequencies of 91.20, 598.02, and 1765.03 Hz for Mode 1, Mode 2, and Mode 3, respectively. The pure epoxy-based CL-CC CFRP composite joint showed enhancements of 7, 9, and 9%, as compared to the joint made only from epoxy-based CC-CFRP composite joints. These results indicate that the CL-CC CFRP composite joint constructed with 1.25 wt% of MWCNTs combined with epoxy has achieved its maximum natural frequency. The frequencies corresponding to Mode 1, Mode 2, and Mode 3 are 108.79, 713.93, and 2001.57 Hz, respectively. These values exceed those of pure epoxy by 19, 19, and 13%, respectively. The natural frequencies of 1.25 wt% MWCNT-based CL-CC CFRP composite joints are 28, 30, and 24% greater than the natural frequencies of

pure epoxy-based CC-CFRP composite joints in the three modes, respectively. The increase in natural frequency is attributed to the addition of MWCNTs, which enhances the stiffness and strength of the composite joint. These results demonstrate the potential for improved performance and durability in structural applications. Furthermore, the enhanced natural frequencies also suggest that the composite joint with MWCNTs is more resistant to vibrations and dynamic loads compared to pure epoxy joints. This indicates a promising direction for future research on advanced materials for structural engineering.

A considerable improvement in the natural frequency was achieved with the use of 1.25 wt% of MWCNT reinforcements with adhesive. The effective incorporation of MWCNTs led to an improvement in the bonding between



**Figure 9:** (a) Mode 1 – natural frequency *versus* wt% of MWCNT content, (b) Mode 2 – natural frequency *versus* wt% of MWCNT content, (c) Mode 3 – natural frequency *versus* wt% of MWCNT content, and (d) plot for damping factor *versus* mode of vibration corresponding to wt% of MWCNT content.

the adherent and the adhesive. Therefore, it functioned as a precise mechanism to ensure the trustworthy bonding of the adhesive substance and the laminate plies that had been co-cured and cured together. It is possible to reduce the natural frequency of the CFRP composite junction by clumping, which is caused by the addition of an excessive amount of MWCNTs to the adhesive. In comparison to other specimens, the damping values of the lap joints that were reinforced with 1.25 wt% of MWCNTs and that were subjected to co-curing were found to be lower. The increased adhesion between the adherend and the adhesive leads to a decrease in the energy dissipation behaviour of the composite joints that have been co-cured. Therefore, it is possible to conclude that the drop in energy dissipation behaviour resulted in a fall in the inherent damping value of composite materials [13]. This suggests that there is an optimal amount of MWCNTs that can be added to the adhesive to maintain desired damping values in composite joints. Further research could explore different reinforcement methods or materials to improve the energy dissipation behaviour without sacrificing damping values.

## 3.3 Microstructural analysis

An FE-SEM instrument developed by Thermo Fisher, FEI Quanta 250 FEG, was used to examine the surface morphology of fracture tested samples. This device relies on a Schottky field-emitting electron cannon as its main electron source. There are a number of unique aspects to this instrument. With a voltage of 30 kV and a high vacuum environment, the apparatus is capable of magnifying objects up to 100,000 times. Its operational voltage range is 5–30 kV. FESEM analysis of fractography followed previous efforts to comprehend flexural surface cracking. A precise cutting instrument was used to carefully trim the specimens to dimensions of 10 mm × 10 mm before analysis. To improve the surfaces' electrical conductivity, they were gilded before scanning.

The presence of uniform and smooth failure surfaces reduced the adhesive's ability to bond with the adherend in specimens without MWCNTs, as shown in Figure 10(a). Because of this, the joint's strength and stability were diminished, and it became more easily damaged. The

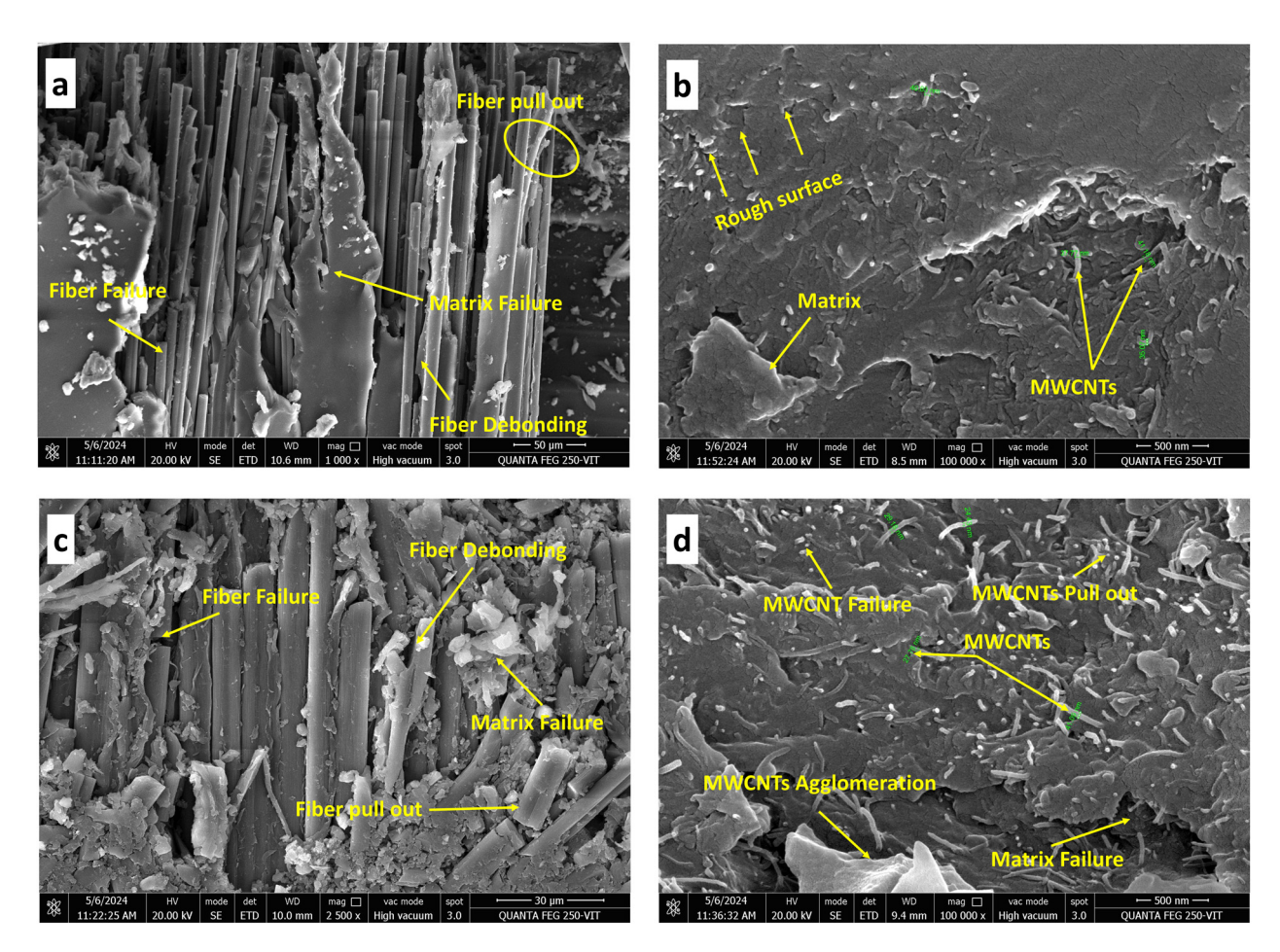


**Figure 10:** FESEM images of the fractured surfaces under a flexural load. (a) Neat CL-CCT, (b) 0.25% of MWCNT CL-CCT, (c) 0.5% of MWCNT CL-CCT, and (d) 0.75% of MWCNT CL-CCT.

presence of MWCNTs in the adhesive zone caused the crack propagation trajectory to change to a longer one, as shown in Figure 10(b). Prolonging the failure process made it easier to reinforce the joint, which in turn enhanced the cohesive force. Through co-curing bonding techniques, a rough surface was formed on both adherends in an overlapping zone. As a result, the flexural strengths between the matrix and the fibre strengthened, and the bond between the two was further solidified. This resulted in improved cohesive and adhesive qualities. The capacity of layers to adhere to one another or interlayer adhesion is essential for bending force resistance because it stops layers from peeling apart and fibres from coming loose. By creating a rough area in the bonding zone and evenly dispersing MWCNTs, the flexural strength of the CL-CC CFRP composite joint was enhanced. Additionally, MWCNTs introduced additional nano-scale toughening mechanisms to adhesives, increasing their fracture resistance. This made adhesive-bonded joints more prone to fracture [45,46].

Figure 10(c) shows that the probability of crack formation and propagation is reduced when there are uneven surfaces close to the bonding region. Increased flexural strength and delayed joint failure were the end outcomes. Due to its emphasis on uniform MWCNT dispersion and strong matrix-MWCNT bonding, the described procedure is effective for co-cured joints. The co-cured joint showed more clusters of nanoparticles as the percentage of MWCNTs increased. This is because MWCNTs increased the joint's strength. Compared to joints devoid of MWCNTs, those reinforced with these nanoparticles showed lower flexural strength and higher stress concentration. Nanoparticle aggregation in the adhesive layer substantially increased the weight percentage, as shown in Figure 10(d). An increase in stress concentration was noted when MWCNTs were present. The co-cured composite joints could only support a certain amount of weight and were thus less likely to fail. From these results, in CL-CC CFRP composite joints, the flexural strength improved by three techniques – co-curing, covered lamina, and matrix modification.

# 4 Statistical analysis

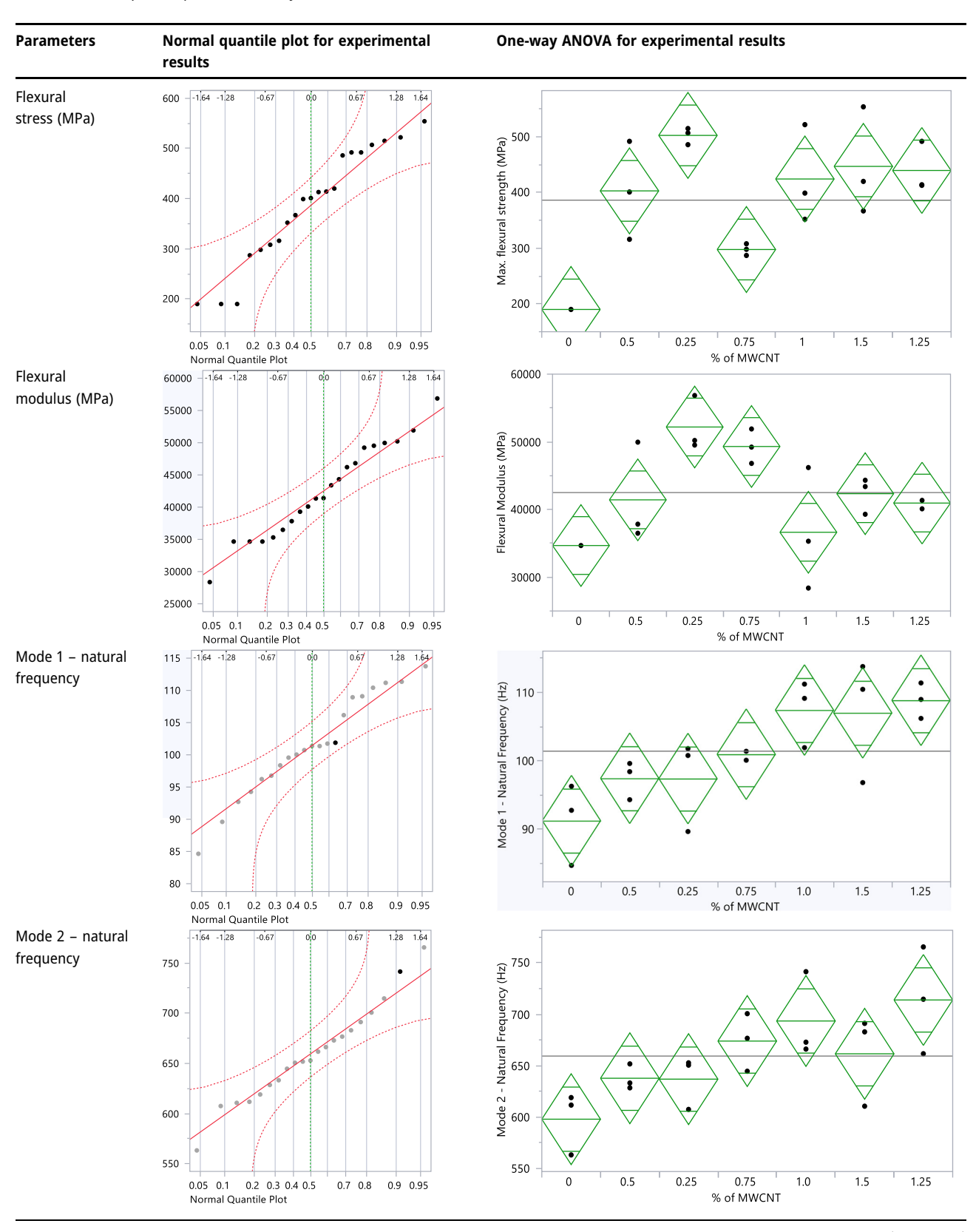
A statistical method was used to analyse the relationships among the means of input and output variables. There are various statistical testing techniques, such as hypothesis testing, confidence intervals, regression analysis, and ANOVA. Based on the categories of independent and dependent variables, the testing techniques were selected. In this research, statistical analyses were performed on every parameter

assessed using JMP Pro 17. The first step of this analysis was to ensure a normal distribution of the data, such as natural frequency across all three modes, flexural strength, and modulus. A normal quantile plot was used. After confirmation of data that were normally distributed, the data were applied to statistical analysis. In this research, independent variables were considered categorical and dependent variables were considered continuous. Due to both dependent and independent variable groups, ANOVA was conducted to examine the flexural strength, flexural modulus, and natural frequency of different modes in CL-CC CFRP composite single-lap joints with varying weight percentages of MWCNT additives. According to the findings presented in Table 1, this analysis indicates that the data conform to a normal distribution. The primary objective of this study was to determine if there were any significant variations in the properties of CFRP single-lap joints with the addition of MWCNTs, specifically in terms of their weights. All attributes examined yielded a P-value below 0.05, as indicated in Table 2. When combined with CL-CC CFRP composite single-lap joints, there is a notable variation in the average weights of the MWCNTs (0, 0.25, 0.75, 1.0, 1.25, and 1.5). This discrepancy is indicated by the 95% confidence level. According to the results, the amount of MWCNTs in the material's weight has a notable impact on its flexural strength, flexural modulus, and natural frequency.

# 5 Prediction using the ANN

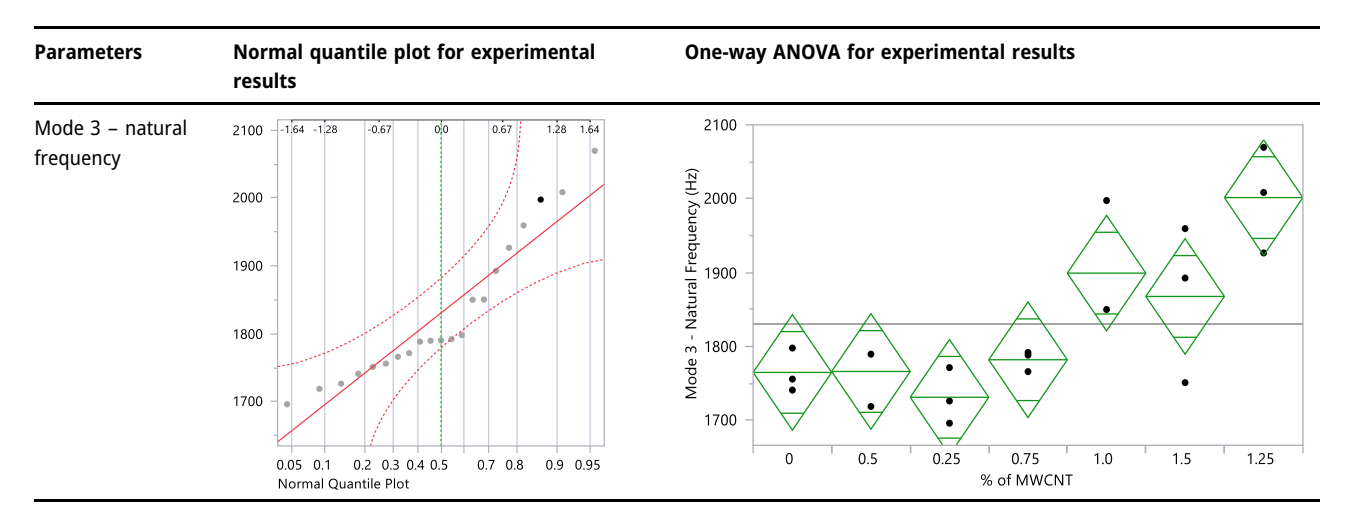
The ANN model faithfully mimics the anatomical and functional features of the real neurological system. For processes that require a high degree of rigidity, like the bending and oscillation properties of CFRP composite joints made of CL-CCT, this performance boost can be quite useful. We must think about how the parameters might affect the material's properties when we choose them. A system of interconnected systems, or neurons, was used to find the best combination of joint depth and reinforcement filler. An input, an output, and a hidden component made up the scheme. As shown in Figure 11(a), a careful analysis of various critical parameters is required to ascertain the number of hidden layers in an ANN. The generated ANN model using the MATLAB ANN tool is shown in Figure 11(b). The intricacies of the subject under examination are of utmost significance. This study highlights the use of complex networks and specialized numerical layers in analysing intricate data patterns and issues. Fifty hidden layers were discovered during this investigation. After conducting numerous tests and evaluations, including training the network on one dataset and

Table 1: Normal quantile plot and one-way ANOVA



14 — Natesan Karthikeyan et al. DE GRUYTER

Table 1: Continued



confirming its functionality on another, this condition was ultimately chosen.

The main consideration behind this decision was the network's capacity to effectively adjust to new information while upholding a well-balanced model complexity. Both the joint depth and weight percentage of MWCNTs are among the four input factors considered in this study. Every parameter on the input layer is controlled by a neuron. Empirical measurements are utilized to train the neural network model and establish the correlation between the input and output data. The input data consist of variables that range from 0 to 1. The eight neurons comprising the output layer are specifically tailored to represent various characteristics of the CL-CCT CFRP composite joints. In addition, these parameters

encompass the maximum flexural strain, maximum flexural strength, flexural modulus, maximum force, deflection, and natural frequencies of the first, second, and third modes.

It randomly divides experimental data to 70% for training, 15% for testing, and 15% for validation. A significant portion of the data is allocated for training purposes, while a smaller portion is reserved for testing and validating the experimental outcomes. Choosing an appropriate cycle number is essential for ensuring reliable training in neural network algorithms. The research utilized a feed-forward back-propagation methodology to predict the vibration behaviour and flexural properties of CL-CCT CFRP composites with adhesively bonded joints. The MATLAB software was employed to achieve this objective.

Table 2: ANOVA of various wt% of MWCNTs of CL-CC CFRP joint specimens

Parameters	Source	Degree of freedom	Sum of squares	Mean square	F	<i>P</i> -value
Flexural stress (MPa)	% of MWCNTs	6	204566.00	34094.3	8.7965	0.0004*
	Error	14	54262.67	3875.9		
	C. Total	20	258828.67			
Flexural modulus (MPa)	% of MWCNTs	6	718,496,834	119,749,472	5.0464	0.0060*
	Error	14	332,214,507	23,729,608		
	C. Total	20	1,050,711,341			
Mode 1 – natural frequency (Hz)	% of MWCNTs	6	773.2106	128.868	4.5147	0.0095*
	Error	14	399.6186	28.544		
	C. Total	20	1172.8292			
Mode 2 – natural frequency (Hz)	% of MWCNTs	6	27267.704	4544.62	3.5749	0.0232*
	Error	14	17797.821	1271.27		
	C. Total	20	45065.524			
Mode 3 – natural frequency (Hz)	% of MWCNTs	6	167893.92	2 27982.3 7.0262 <b>0.0013*</b>		
	Error	14	55755.79	3982.6		
	C. Total	20	223649.72			

Bold values denote statistical significance at the p < 0.05 level.

<sup>\*</sup>A *p*-value less than 0.05 is typically considered to be statistically significant, in which case the null hypothesis should be rejected.

<sup>\*</sup>P-Value greater than 0.05 is not considered to be statistically significant, meaning the null hypothesis should not be rejected.

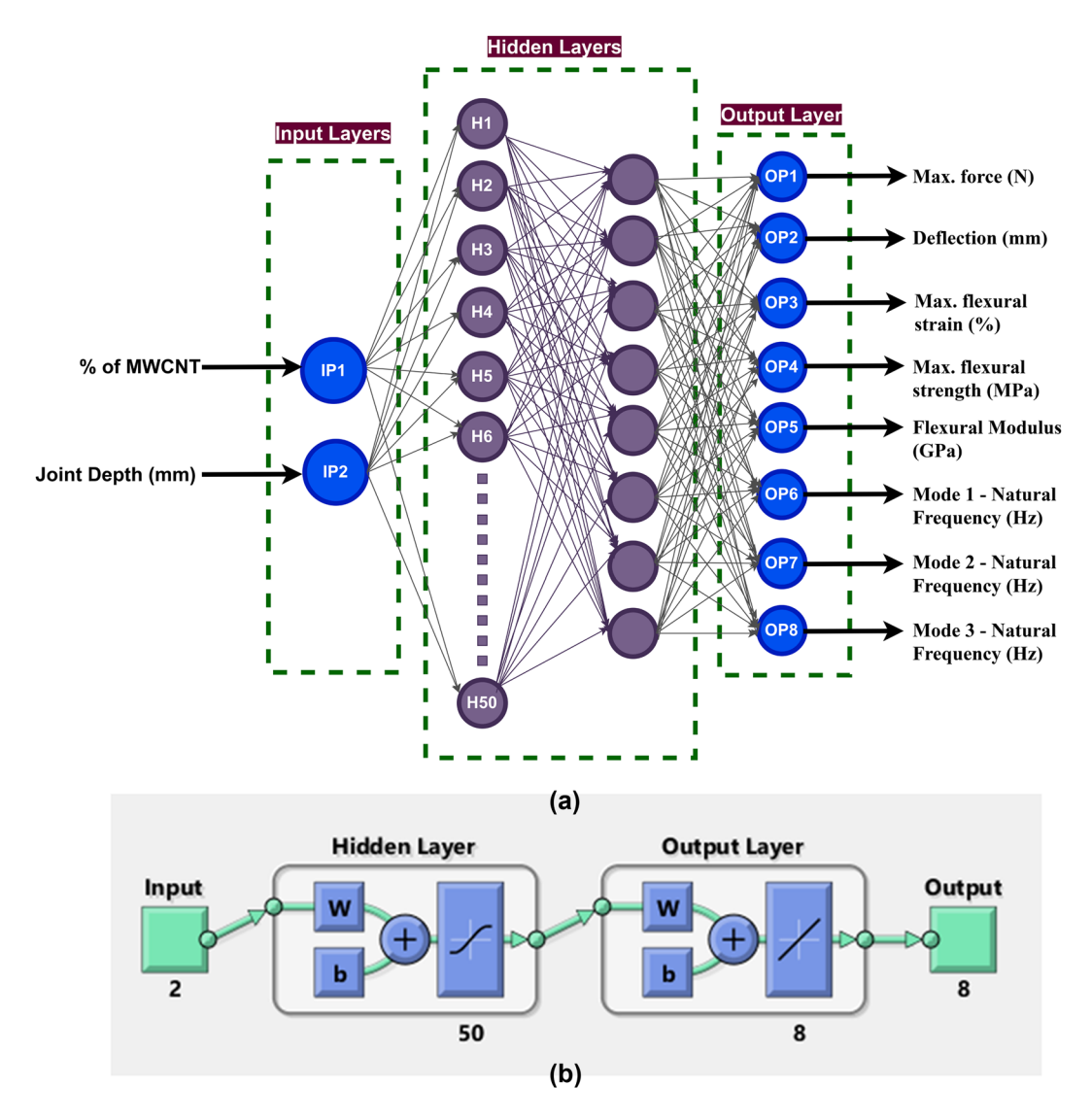
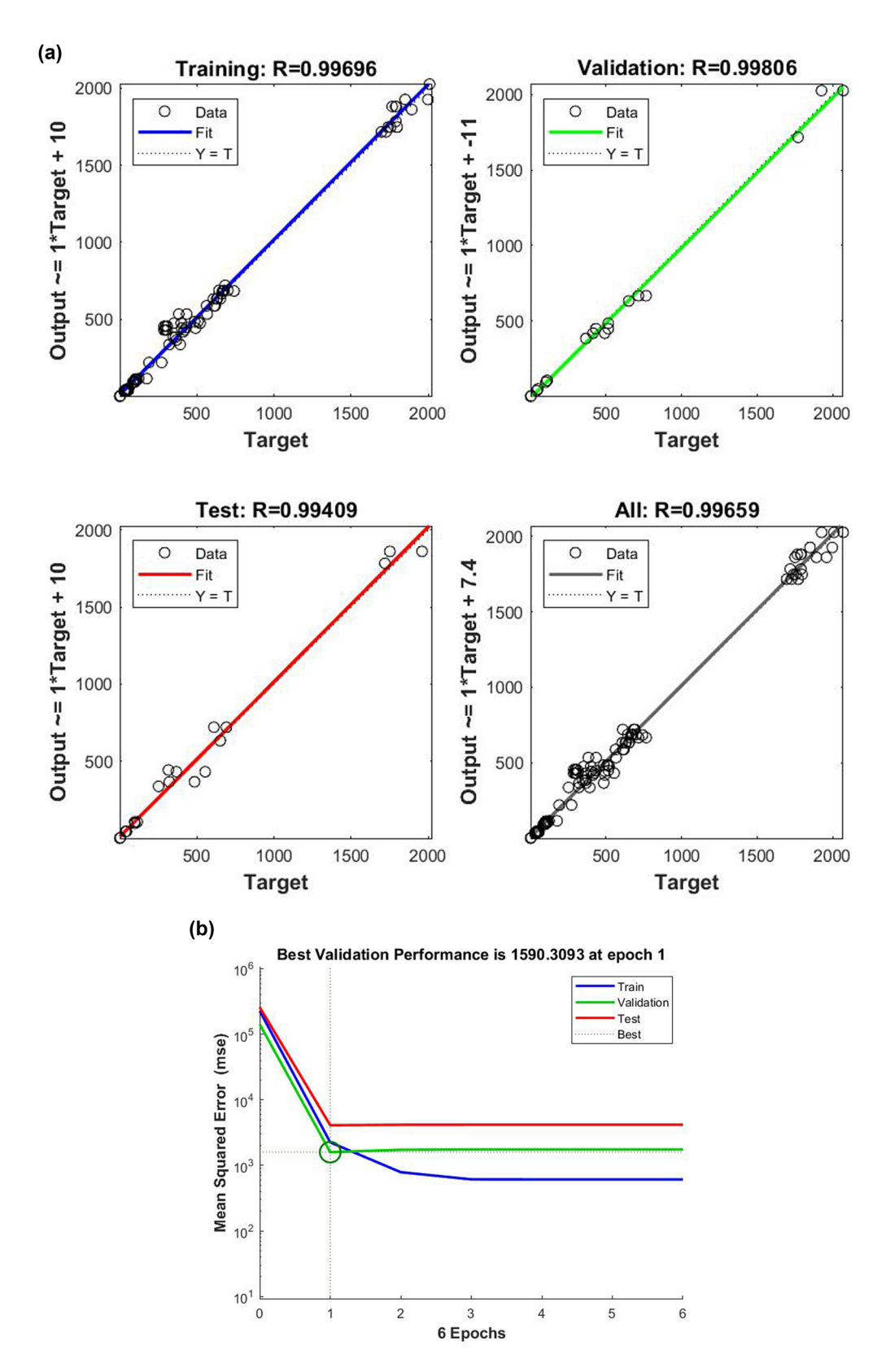


Figure 11: (a) Input and output parameters in the ANN model. (b) Generated ANN model.

Using the Levenberg–Marquardt ANN, linear regression predictions were made, and the percentage error between the network's output and the experimental data was calculated. In Figure 12(a), it is evident that the neural network Levenberg–Marquardt model outperformed the experimental results in the training set. Based on prior research, the model demonstrates a slight improvement compared to other models when considering the validation set. Based on the performance of the validation set, it appears that the developed model has a higher prediction accuracy. The ANN model outperformed other models in this regard. It tested the models' predictive capabilities involved using unseen data. The results indicate that the ANN model demonstrates strong generalization capabilities.

Scatter plots in Figure 12(b) showcase the correlation between the identified output characteristics and the predicted results of the ANN models. Once the coefficient of determination reaches high values for training, validation, testing, and overall, the network is selected for forecasting. These values are R=0.99696, 0.99806, 0.98409, and 0.99659, respectively. Figure 12(b) demonstrates the impressive accuracy of predictions made by models trained using ANNs for the vibration and flexural properties of CL-CCT CFRP composite joints. In addition, the ANN model demonstrates significantly lower error values compared to the existing literature. Table 3 shows that the confirmation of experimental results with ANN predicted results with minimal error.



**Figure 12:** (a) Performance curves of the ANN for predicting the best wt% of MWCNTs and joint depth for their targeted properties and (b) regression analysis of the ANN for predicting the best wt% of MWCNTs and joint depth for their targeted properties.

Table 3: Confirmation of experimental results with ANN predicted results

Factors		Analysis	Output responses							
% of MWCNT	Joint depth (mm)		Max. force (N)	Deflection (mm)	Max. flexural strain (%)	Max. flexural strength (MPa)	Flexural modulus (GPa)	Mode 1 – natural frequency (Hz)	Mode 2 – natural frequency (Hz)	Mode 3 – natural frequency (Hz)
0 2.63	2.63	Experiment	149.50	2.65	0.52	231.00	45.493	91.20	598.02	1765.03
		ANN prediction	140.67	2.703	0.53	217.33	41.886	91.20	598.02	1765.03
		% of error	5.91	2.11	2.10	5.92	7.93	0.00	0.00	0.00
0.25 2.75	2.75	Experiment	358.00	4.75	0.97	502.67	52.186	97.35	636.96	1731.40
		ANN prediction	358.00	4.750	0.97	502.67	52.186	97.35	636.96	1731.40
		% of error	0.00	0.00	0.00	0.00	0.00	0.00	0.00	0.00
0.5 2.91	2.91	Experiment	321.33	4.50	0.97	403.00	41.423	97.39	637.83	1766.30
		ANN prediction	320.00	4.910	1.06	401.00	37.830	94.26	633.21	1789.70
		% of error	0.41	9.11	9.24	0.50	8.67	3.21	0.72	1.32
0.75 3.2	3.25	Experiment	296.00	2.52	0.61	297.67	49.308	100.91	673.97	1782.17
		ANN prediction	296.00	2.515	0.61	297.67	49.308	100.91	673.97	1782.17
		% of error	0.00	0.00	0.00	0.00	0.00	0.00	0.00	0.00
1	3.4	Experiment	461.33	4.64	1.17	424.33	36.631	107.36	693.49	1899.37
		ANN prediction	434.00	4.510	1.13	399.00	35.310	109.07	666.19	1850.40
		% of error	5.92	2.73	3.14	5.97	3.61	1.59	3.94	2.58
1.25	3.34	Experiment	460.00	4.35	1.07	439.67	40.947	108.79	713.93	2001.57
		ANN prediction	473.50	4.495	1.11	452.50	40.721	107.53	688.15	1967.60
		% of error	2.93	3.33	3.42	2.92	0.55	1.16	3.61	1.70
1.5	3.05	Experiment	391.67	4.65	1.05	447.00	42.334	106.96	661.59	1867.83
		ANN prediction	403.50	4.835	1.09	460.50	41.807	105.24	650.92	1855.40
		% of error	3.02	3.90	3.93	3.02	1.25	1.60	1.61	0.67

The bold font indicates the minimum error percentage.

# 6 Conclusions

The purpose of this study is to investigate the effects of adhesive-bonded joints in CL-CC CFRP by employing MWCNTs as a reinforcing agent in a pure epoxy adhesive. To fabricate the joints, a combination of vacuum bag hand layup and covered lamina with co-curing bonding techniques was selected as the method of choice. In addition, the flexural properties were evaluated using a three-point bending test. Furthermore, the vibration characteristics were investigated using a free vibration test that made use of a cantilever beam boundary condition. Based on the investigation, the following assertion can be derived as the inference:

 The flexural strength and modulus of the MWCNT-mixed epoxy adhesive at a weight percentage of 0.25% are significantly higher than those of pure epoxy. Specifically, the flexural strength has increased by 118%, while the modulus has increased by 15%. The addition of MWCNTs enhances the mechanical properties of the epoxy adhesive, making it a promising option for applications requiring high strength and stiffness.

- By incorporating 1.25 wt% of MWCNTs into the epoxy, the vibration characteristics of CL-CC CFRP composite joints were effectively improved. The natural frequencies of Modes 1, 2, and 3 were found to exhibit improvements of 19, 19, and 13%, respectively, when compared to the value of pure epoxy. The addition of MWCNTs also increased the damping ratio of the composite joints, indicating enhanced energy dissipation capabilities. These improvements are crucial for enhancing the overall performance and durability of CL-CC CFRP composite joints in various applications.
- According to the findings of morphological analysis, the bonding that occurred at the interface resulted in an improvement in the flexural properties of the CL-CC CFRP composite joints. Many distinguishable characteristics play a part in determining the bonding property at the interface, as shown in the images obtained from FE-SEM. Several phenomena fall under this category, including crack generation, crack propagation, fibre pullout, and matrix pullout. These phenomena can be influenced by factors such as the surface roughness of materials, the presence of contaminants, and the curing process.

Understanding these interactions is crucial for optimizing the performance of composite joints in various applications.

- A level of confidence of 95% was reached regarding the findings, which demonstrated statistical significance. In situations where the *F*-value is higher than the critical *F*-values and the *p*-value is lower than 0.05, the conclusion can be stated without any reservations. This level of confidence indicates that the results are unlikely to have occurred by chance. Therefore, the findings can be considered reliable and valid for concluding this study.
- The mean squared error values that the ANN produced during the training, validation, and testing phases were *R* = 0.99696, *R* = 0.99806, and *R* = 0.98409, respectively. These values were obtained throughout the program. The overall MSE was achieved at *R* = 0.99659. Based on the findings of the analytical study, it is hypothesized that the application of the ANN methodology could be an exceptionally effective method for predicting outcomes. The consistently high *R*-values obtained during the training, validation, and testing phases indicate a strong performance of the ANN model. This suggests that the ANN methodology has great potential for accurate outcome predictions in future applications.

Acknowledgments: The authors thank the Advanced Vibrations Lab and Composite Lab in the School of Mechanical Engineering, VIT Vellore, for providing access to their facilities. We would also like to acknowledge and thank Universiti Pertahanan Nasional Malaysia (UPNM) for their collaboration and support.

**Funding information:** The authors would like to express gratitude for the financial support from the Universiti Pertahanan Nasional Malaysia (UPNM).

**Author contributions:** All authors have accepted responsibility for the entire content of this manuscript and approved its submission.

**Conflict of interest:** The authors state no conflict of interest.

**Data availability statement:** The datasets generated and/ or analysed during the current study are available from the corresponding author on reasonable request.

## References

 Karthikeyan N, Naveen J. Progress in adhesive-bonded composite joints: A comprehensive review. J Reinf Plast Compos. 2024. doi: 10. 1177/07316844241248236.

- [2] Dhilipkumar T, Rajesh M. Influence of manufacturing process and GFRP pin loading on shear and dynamic behaviour of composite joints. J Adhes. 2023;99:538–57. doi: 10.1080/00218464.2022.2025782.
- [3] Dhilipkumar T, Rajesh M. Enhancing shear strength and structural stiffness of composite joint with carbon nanotube reinforced adhesive through co-bonding technique. J Adhes Sci Technol. 2022;36:2143–57. doi: 10.1080/01694243.2021.2002066.
- [4] Karthikeyan N, Naveen J. Effect of surface modified adherend and nanofiller modified adhesives on the shear behaviour of single lap joints: a mini review. J Adhes Sci Technol. 2024;1–20. doi: 10.1080/ 01694243.2024.2362297.
- [5] Gualberto HR, do Carmo Amorim F, Costa HRM. A review of the relationship between design factors and environmental agents regarding adhesive bonded joints. J Braz Soc Mech Sci Eng. 2021;43:389. doi: 10.1007/s40430-021-03105-2.
- [6] Kaybal HB, Ulus H. Comparative analysis of thermoplastic and thermoset adhesives performance and the influence on failure analysis in jointed elium -based composite structures. Polym Compos. 2024;45:3474–92. doi: 10.1002/pc.28003.
- [7] Tinastepe MT, Kaybal HB, Ulus H, Erdal MO, Çetin ME, Avcı A. Quasi-Static tensile loading performance of Bonded, Bolted, and hybrid Bonded-Bolted Carbon-to-Carbon composite Joints: Effect of recycled polystyrene nanofiber interleaving. Compos Struct. 2023;323:117445. doi: 10.1016/j.compstruct.2023.117445.
- [8] Yildirim C, Ulus H, Beylergil B, Al-Nadhari A, Topal S, Yildiz M. Tailoring adherend surfaces for enhanced bonding in CF/PEKK composites: Comparative analysis of atmospheric plasma activation and conventional treatments. Compos Part A Appl Sci Manuf. 2024;180:108101. doi: 10.1016/j.compositesa.2024.108101.
- [9] Budhe S, Banea MD, de Barros S, da Silva LFM. An updated review of adhesively bonded joints in composite materials. Int J Adhes Adhes. 2017;72:30–42. doi: 10.1016/j.ijadhadh.2016.10.010.
- [10] Venugopal A, Sudhagar PE. Enhancing shear strength of single lap composite adhesive joint with graphene nano-particles and Z-pins reinforcement through co-curing technique. Tribol Int. 2024;195:109636. doi: 10.1016/j.triboint.2024.109636.
- [11] Dhilipkumar T, Rajesh M. Enhancing strength and stiffness of composite joint through co-cure technique. Compos Commun. 2021;27:100878. doi: 10.1016/j.coco.2021.100878.
- [12] Dhilipkumar T, Rajesh M. Multi-scale strengthening of co-cure joints through multiwall carbon nanotube modified adhesive and GFRP pins. Compos Commun. 2022;29:101056. doi: 10.1016/j.coco.2022.101056.
- [13] Dhilipkumar T, Rajesh M. Influence of glass fibre reinforced polymer composite pin reinforcement on shear and dynamic behaviour of composite joint manufactured through co-cure technique. J Compos Mater. 2022;56:1799–809. doi: 10.1177/00219983221088900.
- [14] Layec J, Ansart F, Duluard S, Turq V, Aufray M, Labeau MP.

  Development of new surface treatments for the adhesive bonding of aluminum surfaces. Int J Adhes Adhes. 2022;117:103006. doi: 10. 1016/j.ijadhadh.2021.103006.
- [15] Yudhanto A, Alfano M, Lubineau G. Surface preparation strategies in secondary bonded thermoset-based composite materials: A review. Compos Part A Appl Sci Manuf. 2021;147:106443. doi: 10. 1016/j.compositesa.2021.106443.
- [16] Ejaz H, Saboor D, Bin Sohail MS, Mansoor AH. Effect of various surface treatments on lap shear strength of aluminum adhesive joints. Proceedings of 2022 19th International Bhurban Conference on Applied Sciences and Technology, IBCAST 2022. Institute of Electrical and Electronics Engineers Inc. 2022. p. 76–81. doi: 10. 1109/IBCAST54850.2022.9990536.

- [17] Liu J, Xue Y, Dong X, Fan Y, Hao H, Wang X. Review of the surface treatment process for the adhesive matrix of composite materials. Int J Adhes Adhes. 2023;126:103446. doi: 10.1016/j.ijadhadh.2023.103446.
- [18] Xu LY, Lu JR, Li KM, Hu J. Experimental study of CFRP laser surface modification and bonding characteristics of CFRP/Al6061 heterogeneous joints. Compos Struct. 2022;283:115030. doi: 10.1016/j.compstruct.2021.115030.
- [19] Guo L, Liu J, Xia H, Li X, Zhang X, Yang H. Effect of surface morphology characteristic parameters on the shear strength of aluminum bonded joints. Int J Solids Struct. 2022;238:111420. doi: 10.1016/j.ijsolstr.2022.111420.
- [20] Ou J, Shao Y, Huang C, Bi X. Bond behavior of CFRP sheets-to-steel shear joints with different steel surface treatments. Compos Struct. 2023;322:117376. doi: 10.1016/j.compstruct.2023.117376.
- [21] Safari A, Farahani M, Ghabezi P. Experimental study on the influences of different surface treatment processes and adhesive type on the aluminum adhesive-bonded joint strength. Mech Based Des Struct Mach. 2022;50:2400–13. doi: 10.1080/15397734.2020.1777876.
- [22] Arpitha GR, Mohit H, Madhu P, Verma A. Effect of sugarcane bagasse and alumina reinforcements on physical, mechanical, and thermal characteristics of epoxy composites using artificial neural networks and response surface methodology. Biomass Convers Biorefin. 2023;14:12539–57. doi: 10.1007/s13399-023-03886-7.
- [23] Wang W, Wang Z, Guo R, Xian G. A novel treatment: effects of nanosized and micro-sized  $Al_2O_3$  on steel surface for the shear strength of epoxy–steel single-lap joints. Polymers (Basel). 2022;14(17):3438. doi: 10.3390/polym14173438.
- [24] Yadollahi M, Barkhordari S, Gholamali I, Farhoudian S. Effect of nanofillers on adhesion strength of steel joints bonded with acrylic adhesives. Sci Technol Weld Join. 2015;20:443–50. doi: 10.1179/ 1362171815Y.0000000037.
- [25] Trivedi DN, Rachchh NV. Graphene and its application in thermoplastic polymers as nano-filler – A review. Polym (Guildf). 2022;240:124486. doi: 10.1016/j.polymer.2021.124486.
- [26] Ayatollahi MR, Nemati Giv A, Razavi SMJ, Khoramishad H. Mechanical properties of adhesively single lap-bonded joints reinforced with multi-walled carbon nanotubes and silica nanoparticles. J Adhes. 2017;93:896–913. doi: 10.1080/00218464.2016.1187069.
- [27] Venugopal A, Sudhagar PE. Enhancing shear and flexural strength of single lap composite joints with a graphene nanoparticle-reinforced adhesive through a co-curing technique. Polym Compos. 2023;45(5):4202–20. doi: 10.1002/pc.28053.
- [28] Kumar M, Saini JS, Bhunia H. Investigations on the strength of mechanical joints prepared from carbon fiber laminates with addition of carbon nanotubes. J Mech Sci Technol. 2020;34:1059–70. doi: 10.1007/s12206-020-0208-2.
- [29] Khoramishad H, Ashofteh RS, Mobasheri M, Berto F. Temperature dependence of the shear strength in adhesively bonded joints reinforced with multi-walled carbon nanotubes. Eng Fract Mech. 2018;199:179–87. doi: 10.1016/j.engfracmech.2018.05.032.
- [30] Srivastava VK, Gries T, Quadflieg T, Mohr B, Kolloch M, Kumar P. Fracture behavior of adhesively bonded carbon fabric composite plates with nano materials filled polymer matrix under DCB, ENF and SLS tests. Eng Fract Mech. 2018;202:275–87. doi: 10.1016/j. engfracmech.2018.09.030.
- [31] Ravindran AR, Ladani RB, Wang CH, Mouritz AP. Design considerations in the strengthening of composite lap joints using metal z-pins. Compos Part A Appl Sci Manuf. 2022;160:107031. doi: 10.1016/j.compositesa.2022.107031.
- [32] Campilho RDSG, Pinto AMG, Banea MD, Silva RF, da Silva LFM. Strength improvement of adhesively-bonded joints using a

- reverse-bent geometry. J Adhes Sci Technol. 2011;25:2351–68. doi: 10.1163/016942411X580081.
- [33] Hiremath VS, Reddy MD, Reddy RM, Naveen J, Chand RP. Enhancing shear strength in 3D printed single lap composite joints: A multifaceted exploration of GNP integration, print orientation, utilizing artificial neural networks, and dynamic analysis. J Appl Polym Sci. 2024;141(23):e55469. doi: 10.1002/app.55469.
- [34] Venugopal A, Sudhagar PE. Dual-scale reinforcement of co-cure single lap joints through graphene nanoparticles and CFRP Z-pin. Mater Lett. 2024;370:136833. doi: 10.1016/j.matlet.2024.136833.
- [35] Quan D, Zhao G, Scarselli G, Alderliesten R. Co-curing bonding of carbon fibre/epoxy composite joints with excellent structure integrity using carbon fibre/PEEK tapes. Compos Sci Technol. 2022;227:109567. doi: 10.1016/j.compscitech.2022.109567.
- [36] Tefera G, Bright G, Adali S. Flexural and shear properties of CFRP laminates reinforced with functionalized multiwalled CNTs. Nanocomposites. 2021;7:141–53. doi: 10.1080/20550324.2021.1961507.
- [37] Vijaya Rajan V, Gnanavel BK. An experimental investigation on enhancing the strength and stiffness of GFRP co-cured composite joint: effect of glass powder addition. Mater Res Express. 2022;9:085301. doi: 10.1088/2053-1591/ac8396.
- [38] Mohit H, Sanjay MR, Siengchin S, Kanaan B, Ali V, Alarifi IM, et al. Predicting physico-mechanical and thermal properties of loofa cylindrica fibers and Al<sub>2</sub>O<sub>3</sub>/Al-SiC reinforced polymer hybrid composites using artificial neural network techniques. Constr Build Mater. 2023;409:133901. doi: 10.1016/j.conbuildmat.2023.133901.
- [39] Mohit H, Sanjay MR, Siengchin S, Kanaan B, Ali V, Alarifi IM, et al. Machine learning-based prediction of mechanical and thermal properties of nickel/cobalt/ferrous and dried leaves fiber-reinforced polymer hybrid composites. Polym Compos. 2024;45:489–506. doi: 10.1002/pc.27793.
- [40] Kradinov V, Madenci E, Ambur DR. Application of genetic algorithm for optimum design of bolted composite lap joints. Compos Struct. 2007;77:148–59. doi: 10.1016/j.compstruct.2005.06.009.
- [41] Gowid S, Mahdi E, Alabtah F. Modeling and optimization of the crushing behavior and energy absorption of plain weave composite hexagonal quadruple ring systems using artificial neural network. Compos Struct. 2019;229:111473. doi: 10.1016/j.compstruct.2019.111473.
- [42] Ulus H, Burak Kaybal H. Out-of-plane static loading performance of lightweight aluminum/composite FML structures for retrofitting applications: Effectiveness of bonded, bolted and hybrid bonded/ bolted joining techniques under hydrothermal aging environment. Constr Build Mater. 2023;403:133124. doi: 10.1016/j.conbuildmat. 2023.133124
- [43] Rajesh M, Pitchaimani J. Dynamic mechanical analysis and free vibration behavior of intra-ply woven natural fiber hybrid polymer composite. J Reinf Plast Compos. 2016;35:228–42. doi: 10.1177/ 0731684415611973.
- [44] Rajesh M, Pitchaimani J. Experimental investigation on buckling and free vibration behavior of woven natural fiber fabric composite under axial compression. Compos Struct. 2017;163:302–11. doi: 10. 1016/j.compstruct.2016.12.046.
- [45] Ulus H, Kaybal HB, Cacık F, Eskizeybek V, Avcı A. Effect of long-term stress aging on aluminum-BFRP hybrid adhesive joint's mechanical performance: Static and dynamic loading scenarios. Polym Compos. 2022;43:5301–18. doi: 10.1002/pc.26828.
- [46] Ulus H, Kaybal HB, Cacık F, Eskizeybek V, Avcı A. Fracture and dynamic mechanical analysis of seawater aged aluminum-BFRP hybrid adhesive joints. Eng Fract Mech. 2022;268:108507. doi: 10. 1016/j.engfracmech.2022.108507.